JOURNAL OF AIRCRAFT
Vol. 45, No. 3, May–June 2008

Engineering Notes

ENGINEERING NOTES are short manuscripts describing new developments or important results of a preliminary nature. These Notes should not exceed 2500 words (where a figure or table counts as 200 words). Following informal review by the Editors, they may be published within a few months of the date of receipt. Style requirements are the same as for regular contributions (see inside back cover).

Laminar Flow Separation and Transition on a Low-Reynolds-Number Airfoil

Zifeng Yang* and Hui Hu†
Iowa State University, Ames, Iowa 50011

DOI: 10.2514/1.35051

Introduction

A NUMBER of military and civilian applications require efficient operation of airfoils in low chord Reynolds numbers. The applications include propellers, sailplanes, ultralight man-carrying/man-powered aircraft, high-altitude vehicles, wind turbines, unmanned aerial vehicles, and micro air vehicles. Careful management of boundary layers on low-Reynolds-number airfoils is required to alleviate the deterioration in airfoil performance. Although extensive investigations have been conducted to study laminar flow separation and transition on low-Reynolds-number airfoils, most previous experimental studies were carried out by using single-point-based flow diagnostic techniques such as hot-wire anemometry [1,2] or laser Doppler velocimetry [3,4] to conduct flow measurements. A common shortcoming of single-point-based flow measurements is the incapability of providing spatial correlation of unsteady flow structures to effectively reveal the transient behavior of laminar flow separation. Temporally synchronized and spatially resolved flowfield measurements are highly desirable to elucidate underlying physics to improve our understanding about laminar flow separation and transition on low-Reynolds-number airfoils.

Although several studies have been conducted recently by using the particle image velocimetry (PIV) technique to provide temporally synchronized and spatially resolved flowfield measurements to reveal transient behavior of laminar flow separation on low-Reynolds-number airfoils [5–7], very little in the literature can be found to correlate detailed flowfield measurements with airfoil surface-pressure measurements to gain further insight into the fundamental physics associated with laminar flow separation on low-Reynolds-number airfoils. In the present study, an experimental investigation was conducted to elucidate the underlying physics associated with separation, transition, and reattachment of a laminar boundary layer on a low-Reynolds-number airfoil. In addition to mapping surface-pressure distribution around the airfoil with pressure sensors, a high-resolution PIV system was used to make detailed flow measurements to quantify the occurrence and behavior of laminar boundary-layer separation, transition, and reattachment on the low-Reynolds-number airfoil. The detailed flowfield measurements were quantitatively correlated with the surface-pressure measurements. To the best knowledge of the authors, this is the first effort of its nature. The objective of the present study is to gain further insight into the fundamental physics of laminar flow separation and transition and the evolution of laminar separation bubbles formed on low-Reynolds-number airfoils.

Studied Airfoils and Experimental Setup

The experiments were performed in a closed-circuit low-speed wind tunnel located in the Aerospace Engineering Department of Iowa State University. The tunnel has a test section with a 1.0 by 1.0 ft (30 by 30 cm) cross section and optically transparent walls. The tunnel has a contraction section upstream of the test section, with screen structures and a cooling system installed ahead of the contraction section to provide uniform low-turbulent incoming flow to enter the test section.

The airfoil used in the present study is a NASA low-speed GA(W)-1 airfoil [also labeled as NASA LS(1)-0417]. Compared with standard NACA airfoils, the GA (W)-1 airfoil was specially designed for low-speed general aviation applications with a large leading-edge radius, to flatten the peak in pressure coefficient near the airfoil nose to discourage flow separation [8]. The chord length of the airfoil model is 101 mm (i.e., $C = 101$ mm). The velocity of the incoming flow was set as $U_\infty = 11$ m/s, which corresponds to a chord Reynolds number of $Re_C = 70,000$. The turbulence intensity of the incoming stream was found to be about 1.0%, measured by using a hot-wire anemometer.

The airfoil model is equipped with 43 pressure taps at its median span. The pressure taps were connected to a pressure acquisition system (DSA3217, Scanivalve Corp.) for surface-pressure measurements. The precision of the pressure acquisition system is ±0.2% of the full scale (±10-in. H_2O). A PIV system was used to make flow-velocity-field measurements along the chord at the middle span of the airfoil. The flow was seeded with 1–5-μm oil droplets. Illumination was provided by a double-pulsed Nd:YAG laser (NewWave Gemini 200) emitting two pulses of 200 mJ at the wavelength of 532 nm with a repetition rate of 10 Hz. The laser beam was shaped to a laser sheet (thickness of approximately 1 mm) by using a set of mirrors and spherical and cylindrical lenses. A high-resolution 12-bit (1376×1040 pixel, SensiCam, Cooke Corp.) charge-coupled-device (CCD) camera was used for PIV image acquisition, with its axis perpendicular to the laser sheet. The CCD camera and the double-pulsed Nd:YAG lasers were connected to a workstation via a digital delay generator, which controlled the timing of the laser illumination and the image acquisition. Instantaneous PIV velocity vectors were obtained by using a frame-to-frame cross-correlation technique with interrogation windows of 32×32 pixels. An effective overlap of 50% of the interrogation windows was employed for the PIV image processing. Spanwise vorticity distributions were derived after the instantaneous velocity vectors were determined. Time-averaged quantities such as mean velocity (U, V), turbulent velocity fluctuations $(\bar{u}', \bar{v}')$, normalized Reynolds stress $(\bar{\tau} = -\overline{u'v'}/U_\infty^2)$, and normalized turbulent kinetic energy (TKE) of $\text{TKE} = 0.5 \times (\bar{u}'^2 + \bar{v}'^2)/U_\infty^2$ were obtained from a cinema sequence of 400 frames of instantaneous velocity fields. The measurement-uncertainty level for the velocity vectors is estimated to be within 2% and that of the Reynolds stress and TKE is about 10%.

Received 8 October 2007; revision received 6 December 2007; accepted for publication 26 December 2007.

*Graduate Student, Aerospace Engineering Department.
†Assistant Professor, Aerospace Engineering Department; huhui@iastate.edu. Senior Member AIAA.

Experimental Results and Discussions

Figure 1 shows the mean values of the measured surface-pressure coefficient at the front portion of the airfoil upper surface as the angle of attack (AOA) increases from 4.0 to 14.0 deg. As shown in the figure, the surface-pressure distributions were found to vary significantly at different angles of attack. When the angle of attack is relatively low (i.e., AOA < 8.0 deg), the surface-pressure coefficient profiles were found to reach their negative peaks rapidly at locations quite near to the airfoil leading edge, then recover gradually and smoothly over the upper surface of the airfoil, up to the airfoil trailing edge. As the angle of attack increases to $8.0 \leq \text{AOA} < 12.0$ deg, a distinctive feature of the surface-pressure coefficient profiles is the existence of a region of nearly constant pressure (i.e., pressure-plateau region) at $X/C \approx 0.05$–0.25. Sudden increases in surface-pressure coefficient were found following the plateau regions. Further downstream, surface pressure was found to recover gradually and smoothly, which is similar to those cases with relatively low angles of attack. Such a feature of the surface-pressure coefficient profiles is actually closely related to laminar boundary-layer separation and transition and to formation of laminar separation bubbles on low-Reynolds-number airfoils.

Based on the original ideas proposed by Horton [9], Russell [10] developed a theoretical model to characterize laminar separation bubbles formed on low-Reynolds-number airfoils, which is illustrated schematically in Fig. 2. Russell suggested that a laminar separation bubble formed on a low-Reynolds-number airfoil includes two portions: a laminar portion and a turbulent portion. The location of the pressure plateau would be coincident with that of the laminar portion of the separation bubble. The starting point of the pressure plateau would indicate the location at which a laminar boundary layer separates from the airfoil surface (i.e., separation point). Because the transition of the separated laminar boundary layer to turbulence would result in a rapid pressure rise brought about by fluid entrainment, the termination of the pressure plateau could be used to locate the transition point (i.e., the point at which the transition of the separated laminar boundary layer to turbulence would begin to occur). The pressure rise due to the turbulence transition often overshoots the inviscid pressure that would exist at the reattachment location. Therefore, the location of the point of equality between the actual and inviscid surface pressure marks the location of reattachment (i.e., reattachment point).

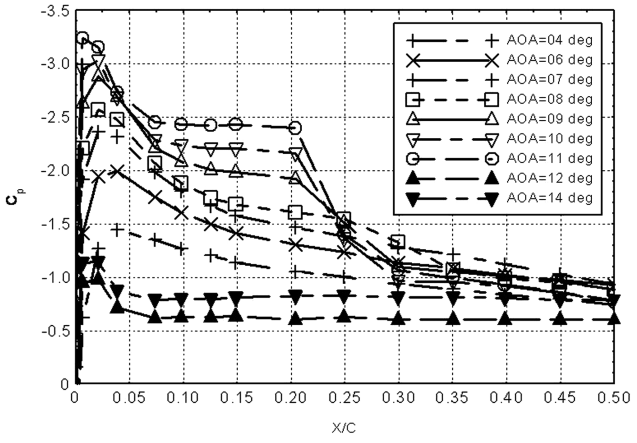

Fig. 1 Measured surface-pressure profiles.

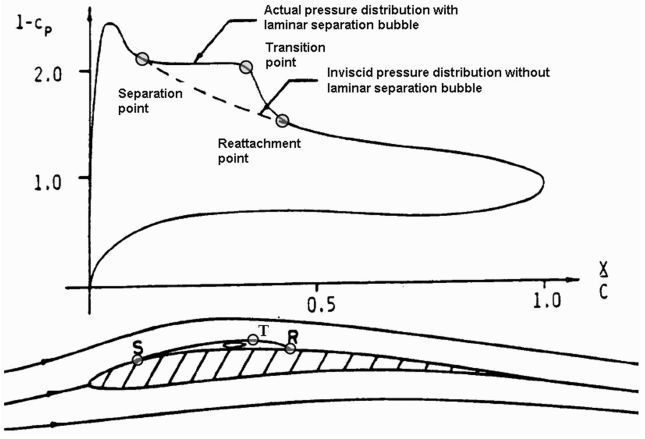

Fig. 2 Typical surface-pressure distribution when a laminar separation bubble is formed on a low-Reynolds-number airfoil (Russell [10]).

Following the work of Russell [10], the locations of critical points (separation, transition, and reattachment points) at different angles of attack were estimated based on the measured airfoil surface-pressure profiles, as given in Fig. 1. A summation of the locations of the critical points is given in Fig. 3. The laminar separation bubble was found to move upstream approaching the airfoil leading edge with increasing angle of attack. The length of the laminar separation bubble (i.e., the distance between the separation and reattachment points) was found to be about 20% of the airfoil chord length, which is almost independent of the angle of attack. As the angle of attack increased, the laminar portion of the separation bubble (i.e., between the separation points and the transition points) was found to be stretched, whereas the turbulent portion (i.e., between the transition points and the reattachment points) was found to become shorter and shorter.

As shown in Fig. 1, the surface pressure over the airfoil upper surface was found to be nearly constant, with the magnitude of the negative surface pressure being significantly reduced at AOA ≥ 12.0 deg. Such surface-pressure distribution indicates that large-scale flow separation has occurred over almost the entire upper surface of the airfoil; that is, the airfoil was found to stall at AOA ≥ 12.0 deg.

With the findings derived from the airfoil surface-pressure measurements in mind, PIV measurements were carried out to provide further insight about the transient behavior of laminar flow separation and transition on the airfoil. In the present study, PIV measurements were conducted at two spatial resolution levels: a coarse level to visualize global features of laminar flow separation, with the measurement window being about 40×25 mm, and a refined level to elucidate details about turbulence transition and reattachment of separated boundary layer, with the measurement window size of about 16×10 mm. The effective resolution of the PIV measurements (i.e., grid sizes) is $\Delta/C = 0.0047$ and 0.0019, respectively, for the coarse and refined levels.

Figure 4 shows the PIV measurements to visualize the global features of a laminar separation bubble formed on the airfoil at AOA $= 10.0$ deg. A laminar boundary layer was revealed clearly as a thin vortex layer affixing to the airfoil surface in the instantaneous PIV measurement results. The laminar boundary layer was found to attach to the airfoil upper surface near the airfoil leading edge, as

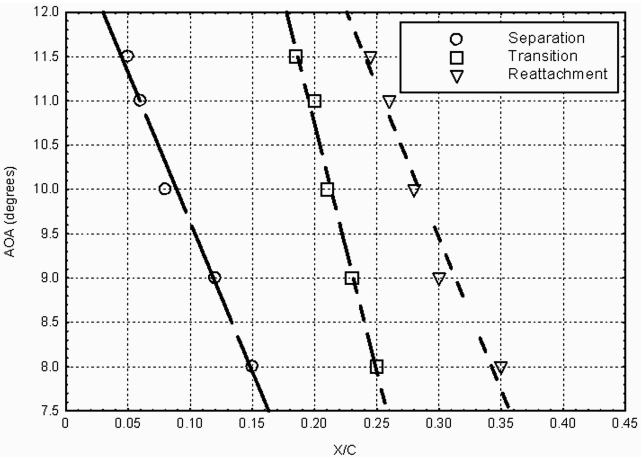

Fig. 3 Locations of critical points vs AOA.

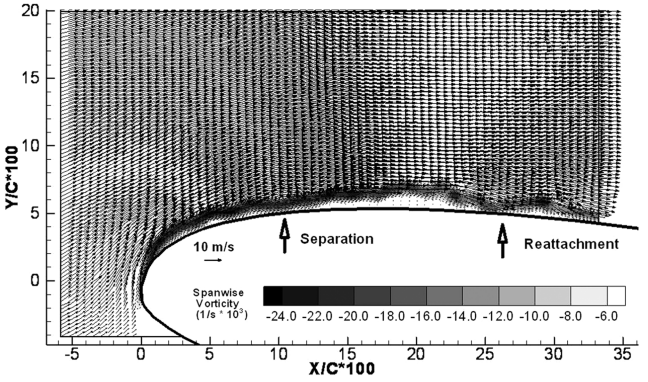

a) A typical instantaneous PIV measurement result

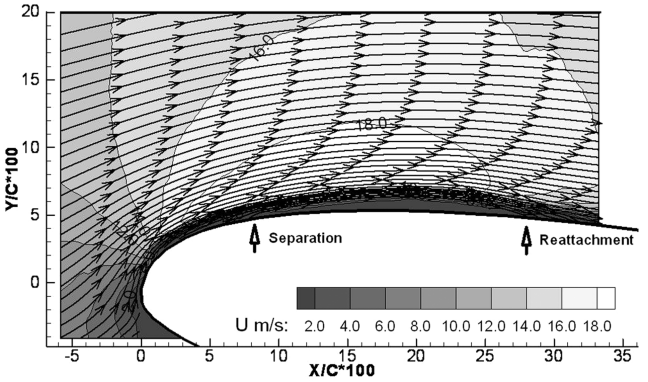

b) Streamlines of the mean flowfield

Fig. 4 PIV measurement results at AOA = 10.0 deg.

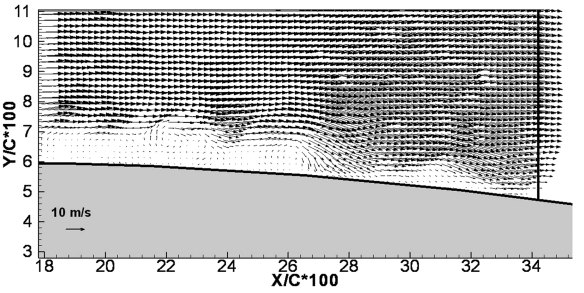

a) A typical instantaneous PIV measurement result

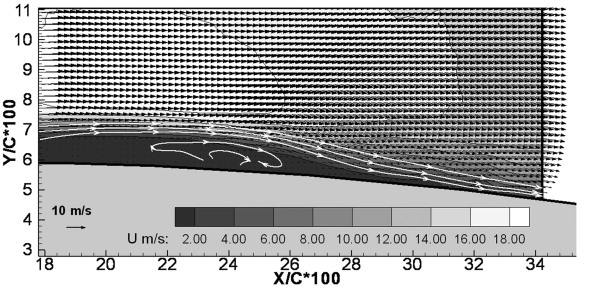

b) Ensemble-averaged PIV measurement results

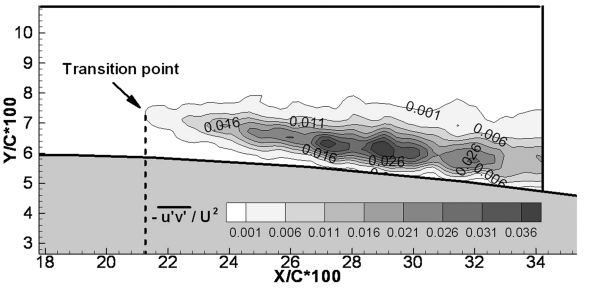

c) Normalized Reynolds stress distribution

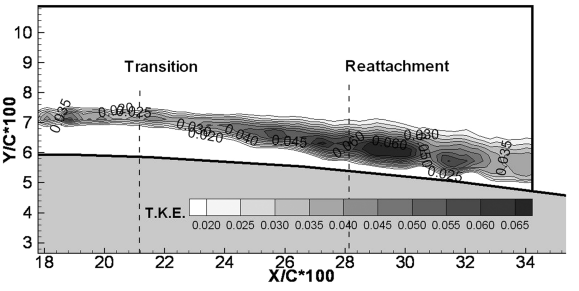

d) Normalized turbulent kinetic energy distribution

Fig. 5 Refined PIV measurements at AOA = 10.0 deg.

expected. Because of the severe adverse pressure gradient at AOA = 10.0 deg, the laminar boundary layer (i.e., the thin vortex layer) was found to separate from the airfoil upper surface at first, then reattach to the airfoil surface at a downstream location, which results in the formation of a separation bubble between the separation point and the reattachment point. A time sequence of instantaneous PIV measurements reveals clearly that, whereas the locations of the separation points and reattachment points varied dynamically from one frame to another, most of the separation points were found to be located at $X/C \approx 0.05$–0.10 and the reattachment points were located at $X/C \approx 0.25$–0.30 at AOA = 10.0 deg. The formation of the separation bubble can be seen more clearly from the streamlines of the mean flowfield. Based on the ensemble-averaged PIV measurement results, the location of the separation point (i.e., the point at which the streamlines of the mean flow would separate from the airfoil upper surface) was found to be in the neighborhood of $X/C \approx 0.08$, which agrees well with the starting point of the pressure plateau in the measured airfoil surface-pressure profile at AOA = 10.0 deg. The reattachment point (i.e., the point at which the separated streamline would reattach to the airfoil upper surface) was found to be located at $X/C \approx 0.28$, which also agrees well with the estimated location of the reattachment point based on the airfoil surface-pressure measurements shown in Fig. 3. Although the total length of the separation bubble was found to be about 20% of the airfoil chord length, the separation bubble was found to be very thin: only about 1% of the chord length in height.

The refined PIV measurement results given in Fig. 5 provide further insight into the fundamental physics associated with turbulent transition and reattachment of the separated laminar boundary layer. Although the laminar boundary layer was found to separate from the airfoil upper surface in the neighborhood of $X/C \approx 0.05$–0.10 at AOA = 10.0 deg, the instantaneous PIV measurement results given in Fig. 5a clearly show that the separated laminar boundary layer would transit to turbulence rapidly by generating unsteady vortex structures. The separated laminar boundary layer was found to behave like a free shear layer, and rolling up of unsteady vortex structures due to the Kelvin–Helmholtz instabilities and transition to turbulent flow would be readily realized. After transition to turbulence, the increased entrainment of turbulent flow could make the separated boundary layer reattach to the airfoil upper surface as a turbulent boundary layer at AOA = 10.0 deg, which consequently results in the formation of a laminar separation bubble on the airfoil. The reattachment of the separated boundary layer to the airfoil upper surface and consequent formation of the separation bubble are revealed more clearly in the ensemble-averaged velocity field and corresponding streamlines given in Fig. 5b.

Figure 5c shows the contour lines of the measured normalized Reynolds stress above a critical value of 0.001. This critical value has been chosen widely in the literature to locate the onset of turbulent transition of separated laminar boundary layers [2,5,7]. Following the work of Burgmann et al. [7], transition onset position was estimated as the streamwise location at which the normalized Reynolds stress first reached the value of 0.001. Therefore, transition position was identified to be located at $X/C \approx 0.21$ at AOA = 10.0 deg based on the PIV measurements. The transition point identified from the PIV measurement results was found to agree well

with the estimation based on the airfoil surface-pressure measurements at AOA = 10.0 deg, which is given in Fig. 3.

The measured TKE distribution given in Fig. 5d reveals that the regions with higher turbulent kinetic energy were confined in a thin layer upstream of the transition point, due to the laminar nature of the separated boundary layer. The regions with higher turbulent kinetic energy were found to become much wider after the turbulence transition of the separated laminar boundary layer (i.e., downstream of the transition point). The regions with higher turbulent kinetic energy were found to be quite close to the airfoil surface downstream of the reattachment point (i.e., $X/C \geq 0.28$). It indicates that the reattached turbulent boundary layer is much more energetic and therefore much more capable of advancing against an adverse pressure gradient without flow separation, compared with the laminar boundary layer upstream of the separation bubble. As a result, the reattached turbulent boundary layer was found to stay attached to the airfoil surface firmly, from the reattachment point up to the trailing edge of the airfoil.

PIV measurement results not shown here clearly reveal that the separation bubble would burst, causing airfoil stall, when the adverse pressure gradient became too significant at AOA > 12.0 deg. Although the laminar boundary layer was found to separate from the airfoil upper surface very near to the airfoil leading edge and to transit to turbulence rapidly, the separated boundary layer was found to be lifted and expelled far away from the airfoil upper surface, due to a much more significant adverse pressure gradient at AOA $\geq$ 12.0 deg. The separated boundary layer could not reattach to the airfoil surface any more. As a result, large-scale flow separation was found to take place over almost the entire upper surface of the airfoil; that is, the airfoil was found to stall at AOA $\geq$ 12.0 deg.

Conclusions

An experimental study was conducted to characterize the transit behavior of laminar flow separation and transition on a low-speed NASA GA(W)-1 airfoil at $Re_C = 70,000$. In addition to mapping surface-pressure distribution around the airfoil, a high-resolution PIV system was used to make detailed flowfield measurements to quantify the occurrence and behavior of laminar boundary-layer separation, transition, and reattachment at various angles of attack (AOA). The detailed flowfield measurements were correlated with the surface-pressure measurements to elucidate the underlying physics associated with the separation, transition, and reattachment processes of the laminar boundary layer. The measurement results revealed clearly and quantitatively that laminar boundary layer would separate from the airfoil surface as the adverse pressure gradient over the airfoil upper surface became severe at AOA $\geq$ 8.0 deg. The separated laminar boundary layer was found to transit to turbulence rapidly by generating unsteady Kelvin–Helmholtz vortex structures. The separated boundary-layer flow reattached to the airfoil surface as a turbulent boundary layer when the adverse pressure gradient was adequate at 8.0 $\leq$ AOA< 12.0 deg, resulting in the formation of a laminar separation bubble on the airfoil. The reattached turbulent boundary layer was found to be more energetic and thus more capable of advancing against an adverse pressure gradient without flow separation, compared with the laminar boundary layer upstream of the laminar separation bubble. The separation bubble was found to be about 20% of the airfoil chord in length and only about 1% of the cord length in height. Although the separation bubble was found to move upstream approaching the airfoil leading edge with increasing angle of attack, the total length of the separation bubble was found to be almost independent of the angle of attack. Although the laminar portion of the separation bubble was found to be stretched, the turbulent portion became shorter with increasing angle of attack. The locations of the critical points (separation, transition, and reattachment points) identified from the PIV measurements were found to agree with those estimated based on the airfoil surface-pressure measurements. The separation bubble was found to burst, causing airfoil stall, when the adverse pressure gradient became too significant at AOA $\geq$ 12.0 deg.

Acknowledgments

The authors want to thank P. Sarkar, F. Haan, and B. Rickard of Iowa State University for their help in conducting the experiments. The support of the National Science Foundation CAREER program under award CTS-0545918 is gratefully acknowledged.

References

[1] Hatman, A., and Wang, T., "A Prediction Model for Separated Flow Transition," *Journal of Turbomachinery*, Vol. 121, No. 3, 1999, pp. 594–602.

[2] Volino, R. J., and Hultgren, L. S., "Measurements in Separated and Transitional Boundary Layers Under Low-Pressure Turbine Airfoil Conditions," *Journal of Turbomachinery*, Vol. 123, No. 2, 2001, pp. 189–197. doi:10.1115/1.1350408

[3] Fitzgerald, E. J., and Mueller, T. J., "Measurements in a Separation Bubble on an Airfoil Using Laser Velocimetry," *AIAA Journal*, Vol. 28, No. 4, 1990, pp. 584–592.

[4] O'Meara, M. M., and Mueller, T. J., "Laminar Separation Bubble Characteristics on an Airfoil at Low Reynolds Numbers," *AIAA Journal*, Vol. 25, No. 8, 1987, pp. 1033–1041.

[5] Ol, M. V., Hanff E., McAuliffe, B., Scholz, U., and Kaehler, C., "Comparison of Laminar Separation Bubble Measurements on a Low Reynolds Number Airfoil in Three Facilities," AIAA Paper 2005-5149, June 2005.

[6] Raffel, M., Favier, D., Berton, E., Rondot, C., Nsimba, M. and Geissler, M., "Micro-PIV and ELDV Wind Tunnel Investigations of the Laminar Separation Bubble Above a Helicopter Blade Tip," *Measurement Science and Technology*, Vol. 17, No. 7, 2006, pp. 1652–1658. doi:10.1088/0957-0233/17/7/003

[7] Burgmann, S., Brücker, S., and Schröder, W., "Scanning PIV Measurements of a Laminar Separation Bubble," *Experiments in Fluids*, Vol. 41, No. 2, 2006, pp. 319–326.

[8] McGee, R. J., and Beasley, W. D., "Low-Speed Aerodynamics Characteristics of a 17-Percent-Thick Airfoil Section Designed for General Aviation Applications," NASA TN D-7428, December, 1973.

[9] Horton, H. P., "A Semi-Empirical Theory for the Growth and Bursting of Laminar Separation Bubbles," Aeronautical Research Council, CP 1073, London, June 1969.

[10] Russell, J., "Length and Bursting of Separation Bubbles: A Physical Interpretation," *Science and Technology of Low Speed and Motorless Flight*, CP2085, Part 1, NASA Langley Research Center, Hampton, VA, 1979, pp. 177–202.